

# Simulation of plasmonic effects of Metal (Au,Ag and Al) NPs and rGO embedded in aqueous solutions

Vladan Stojkovic<sup>a</sup>, Paula Louro<sup>a,b</sup>

<sup>a</sup> Electronics Telecommunication and Computer Dept. ISEL/IPL, R. Conselheiro Emídio Navarro, 1, 1949-014 Lisboa, Portugal,

<sup>b</sup> CTS-UNINOVA, Quinta da Torre, Monte da Caparica, 2829-516, Caparica, Portugal.  
[42437@alunos.isel.ipl.pt](mailto:42437@alunos.isel.ipl.pt) [plouro@deetc.isel.ipl.pt](mailto:plouro@deetc.isel.ipl.pt)

**Abstract – Graphene [1] is a material that has been extensively explored in recent years as a material with optical properties that enable its application as active material in sensing devices.**

**In this work we will study plasmonic effects and optical properties of graphene and metal nanoparticles (AuNPs), comparing its results, whenever possible, with results obtained in previous studies. Analysis will be supported by simulation results obtained with Matlab (“Mie analysis”).**

**Keywords: Graphene, graphene oxide; reduced graphene oxide, silicon, Au, Ag, Al, Mie analysis, LSPR, plasmonics.**

## I. INTRODUCTION

Carbon [2] nanomaterials such as Graphene, Graphene Oxide (GO) and Reduced Graphene Oxide (rGO) have been extensively studied in recent times as promising materials for several important applications, mainly due to their excellent physical and chemical properties. On the other hand, metal plasmonic nanostructures, such as gold (Au) nanoparticles (NP), have been widely used due to their excellent optical properties.

These two materials, rGO and Au, are attractive due to the possibility of easy molecules bonding of to their surfaces, and to the localized surface plasmon resonance phenomenon (LSPR). LSPR is related to electromagnetic modes caused by electron oscillations of noble metal nanoparticles embedded in a dielectric medium.

Among the optical properties, the excitation by electromagnetic radiation of metallic nanostructures smaller than the wavelength of incidence light causes the radiation electric field to engage with collective electronic oscillations. When the incidence frequency equals the natural resonant frequency of the electronic density oscillation in the material, the oscillations are maximized, inducing the formation of intense local electric fields in the vicinity of the nanoparticle. These fields themselves act on the electrons by reinforcing the oscillations, leading to the LSPR phenomenon.

Through nanoparticles, therefore, it is demonstrated that it is possible to manipulate and benefit from optics at nanometer scales, making common optical fields capable of producing strong evanescent waves confined to nanoparticle dimensions.

One of the important scientific areas in which these phenomena and nanomaterials can be applied is sensors and biosensors. Detection of chemical compounds and biological structures is of great importance in various

sectors of human activity, especially in the health field, such as medical diagnosis.

Thus, the purpose of this work is to deepen the study of graphene, in the form of reduced graphene oxide nanocomposite (RGO) and gold nanoparticles (NP), using transmission/reflection analysis technique of light. As the final objective goes beyond this work, an evaluation of the potential of this nanocomposite for future use as a functional element in biosensors will be developed.

The plasmonic properties of RGO nanocomposite with metal NP (Au, Ag and Al) will be simulated as a function of the size and simulations will be used to evaluate whether their combined characteristics can be efficiently employed in the field of biosensors.

## II. WHAT IS GRAPHENE?

Graphene was discovered in 2004 by researchers at the University of Manchester, a work that awarded them the Nobel Prize in physics in 2010 [3].

The term Graphene was adopted in 1962, from the junction of graphite with the suffix -ene, due to the existing double bond. It consists of a flat monolayer of carbon atoms, organized into hexagonal cells with sp<sup>2</sup> hybridized atoms, resulting in a free electron per carbon atom in the p-orbital and making graphene a usable material for various applications [4].

This unique structure gives Graphene several superior properties such as high electrical and thermal conductivity, good transparency, good mechanical strength, inherent flexibility and very high specific surface area.

The electrical conductivity (up to  $2 \times 10^4$  S/cm) and high electronic mobility ( $2 \times 10^5$  cm<sup>2</sup>/V s, which is more than 100 times higher than silicon) in the graphene monolayer result from a small effective mass. Electrons in a solid are restricted to certain energy bands. In an insulator or semiconductor, an electron attached to an atom can be released only if it gets enough energy to jump the gap between the valence and the conduction band. But in graphene the difference between these two bands is infinitesimal, which explains why graphene electrons can move very easily and quickly. Thus, electrons in a single graphene layer behave as massless particles moving at a speed of approximately  $10^6$  m/s. It is the thinnest material ever known and the strongest ever measured in the universe, has an extremely high Young modulus (1 TPa) and the highest intrinsic resistance (approximately 130 GPa) ever measured.

The thermal conductivity of graphene at room temperature can reach 5000 W/mK (comparatively speaking it can be mentioned that copper is 400 W/mK), which enhances its applicability in thermal control. It has a very high surface area (2600 m<sup>2</sup>/g), much larger than the surface areas of graphite (10 m<sup>2</sup>/g) and carbon nanotubes (1300 m<sup>2</sup>/g).

In Table I main electrical properties of graphene are summarized.

TABLE I  
PROPERTIES OF GRAPHENE [4].

Transmittance	~97.7 %
Absorbance	2.3 %
Density	0.77 mg m <sup>-2</sup>
Charge carrier density	10 <sup>12</sup> cm <sup>-2</sup>
Resistivity	10 <sup>-6</sup> Ω cm
Surface area	2630 m <sup>2</sup> g <sup>-1</sup>
Stiffness Young modulus	1110 GPa
Strength	125 GPa
Thermal conductivity	5000 Wm <sup>-1</sup> K <sup>-1</sup>
Electrical mobility	200000 cm <sup>2</sup> V <sup>-1</sup> s <sup>-1</sup>

In relation to optical properties, graphene has an almost total transparency. It can absorb a fraction of 2.3% of light (Table 1). Its optical properties are strongly related to its electronic properties as well as its low energy electronic structure.

These properties (Table 1), provide graphene as a material that can be used in applications ranging from polymeric materials to sensors, transistors, portable electronic devices and electrochemical energy storage systems.

Among the most promising materials in the field of biosensors stand out two variants of graphene: graphene oxide (GO) and reduced graphene oxide (rGO) [5][6]. Both materials, GO and rGO, are able to be mixed with nano materials, such as noble materials like gold (Au) and silver (Ag) and enhance their resonant plasmonic capacities.

### III. LSPR

Localized Surface Plasmon Resonance (LSPR) is an optical phenomenon that occurs in NP's smaller than the electromagnetic wavelength of the incident light [7][8][9][10], as shown in Figure 1.

An electromagnetic wave (light) can excite the electrons located in the valence band of the noble metals, so that there is a transition of electrons from valence band energy level to conduction band level. At the initial moment there is the displacement of electrons in the opposite direction to the electric field of the incident wave (Figure 1).

This displacement of charges promotes the induction of an electric dipole in the particle. The induced dipole promotes the appearance of a restorative electric field in NP, which has the function of restoring the equilibrium given by the distortion of the charges. This restorative force and dipole induction, when connected, generate the plasmon resonance.

The cloud around the NP has its own oscillation and will have maximum oscillation when the incoming wave is at the resonant cloud oscillation frequency.

Thus, plasmon in an NP can be considered as a harmonic oscillator driven by the resonant light wave, where the electron cloud oscillates as a simple dipole in the direction parallel to the electric field of electromagnetic radiation. Only the wave often resonant with cloud oscillation is capable of producing the LSPR phenomenon.

Localized surface plasmon resonance is influenced by the size of NP, its geometry (involves changing the energy conditions on its surface), the change of local dielectric conditions surrounding the NP, as well as the type of ligand (nanoparticle-interacting molecules that can change the dielectric constant) and solvent type (which also changes the dielectric constant).

It is due to the plasmon resonance phenomena in noble metals that we are able to use the UV-Vis spectroscopy technique and the induced changes in the plasmon oscillation frequency caused by the change in the surrounding dielectric constant. The presence of ligands and solvents also cause dielectric constant changes and alter plasmon resonance conditions.

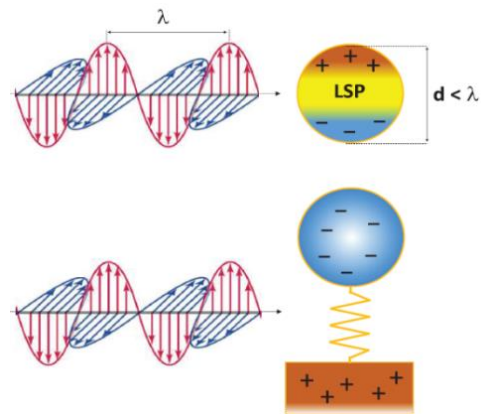


Fig. 1. Incidence of light over metallic NP and oscillator model [11].

### IV. MIE THEORY

In 1908 Gustavo Mie presented a satisfactory resolution for Maxwell's equations, through extensive mathematical work done by hand, in which he considered an electromagnetic wave interacting with a conducting sphere [11].

In this work, Mie conditioned the system under the following boundary conditions: a polarized electromagnetic wave on a given plane falling on a homogeneous sphere surrounded by a real dielectric medium, with equivalent real refractive index (Re). Considering the conducting sphere, the phenomenon of absorption of the electromagnetic wave should be evaluated, since the dielectric function of a conductor is complex (it has an imaginary component, Im) and, in turn, has a complex refractive index, which is a function of the frequency of the incident electromagnetic wave.

Considering only nanoparticles that have  $2r \ll \lambda$  or approximately  $2r < \lambda_{\max}/10$ , and using an approximation known as quasi-static approximation (since the electric field of the incident electromagnetic wave is considered to be static over the nanoparticle over a given period), Mie

obtained the expression for the light extinction cross-section, described in Equation 1 [12][13]:

$$\sigma_{ext} = 9 \frac{\omega}{c} \epsilon_m^{3/2} V \frac{\epsilon_2(\omega)}{[\epsilon_1(\omega) + 2\epsilon_m]^2 + \epsilon_2(\omega)^2} \quad (1)$$

where  $V$  is the volume of the particle,  $\omega$  is the angular frequency of extinguished light,  $c$  is the speed of light, and  $\epsilon_m$  and  $\epsilon_{np}(\omega) = \epsilon_1(\omega) + i\epsilon_2(\omega)$  are the dielectric functions of the medium and nanoparticle (the material), respectively. The resonance condition is reached when:

$$\epsilon_1(\omega) = -2\epsilon_m \quad (2)$$

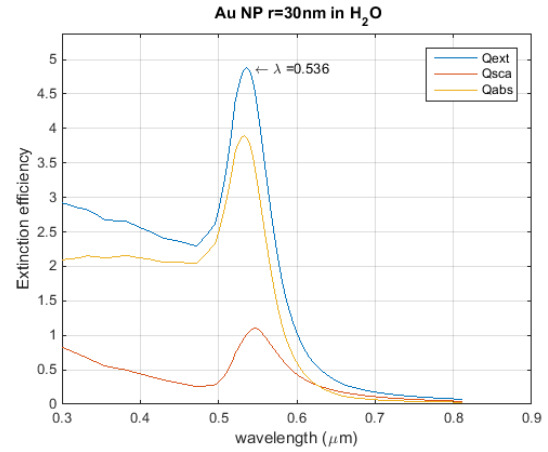
From Equations 1 and 2, we can conclude that the plasmonic properties of any material are defined by their dielectric function  $\epsilon_{np}(\omega)$ . We can also predict that the growth of  $\epsilon_m$  leads to an increase in the negative value of  $\epsilon_1$ , which is necessary to satisfy resonance conditions. This shifts the plasmonic peak to the infrared side, which corresponds to increase the wavelength. From the physical point of view, this increase in  $\epsilon_m$  corresponds to an increase of the restorative force in the polarized electron cloud, which in turn lowers the LSPR frequency. We can conclude that LSPR is very sensitive to changes in the surrounding environment,  $\epsilon_m$ , of NP (or change in the refractive index of the medium). We can also infer that  $\sigma_{Ext}$  depends on the particle volume.  $\sigma_{Ext}$  is maximum when the denominator is minimized, i.e., when plasmon is excited at the frequency that satisfies the condition  $\epsilon_1(\omega) = -2\epsilon_m$ , resulting in a sharp increase in absorption and/or scattering at that wavelength.

## V. SIMULATIONS

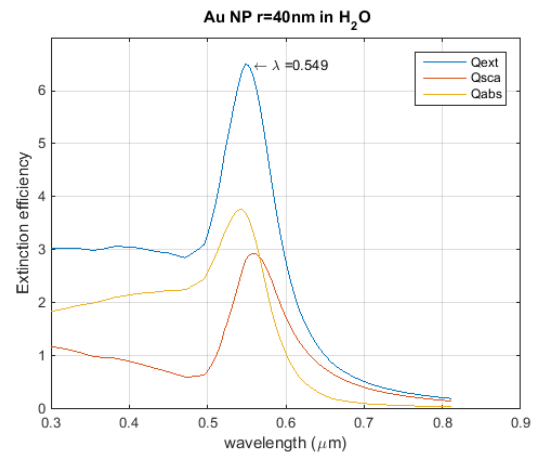
In this section we present simulation results developed in MatLab for the evaluation of the extinction efficiency, predicted by the Mie theory, as a function of the light wavelength. We used three different materials for the embedded nanoparticles (Au, Ag and Al) in different media (water, rGO matrix). It was analyzed the influence of the NP particle size and of the particle's embedding medium.

### 1. Influence of gold NP size in water

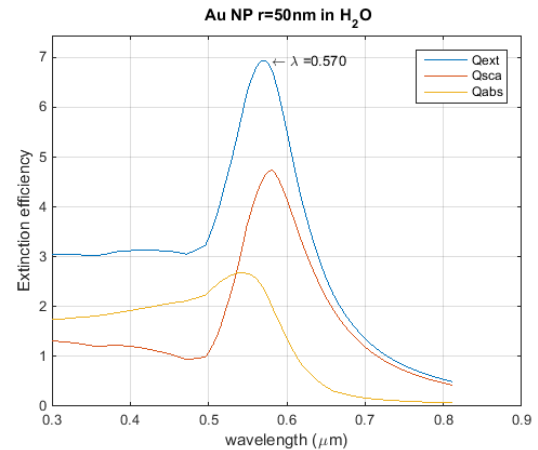
In Figure 2 it is displayed the simulated extinction coefficient variation with light wavelength for gold NP of sizes ranging from 30 nm up to 70 nm. It was assumed that NP were embedded in water. The wavelength range varied from 300 nm up to 900 nm.



a)



b)



c)

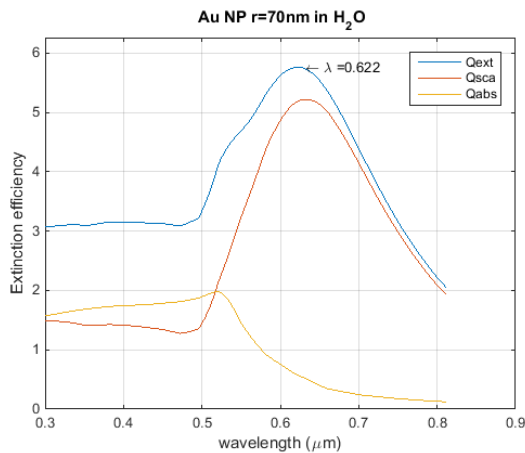
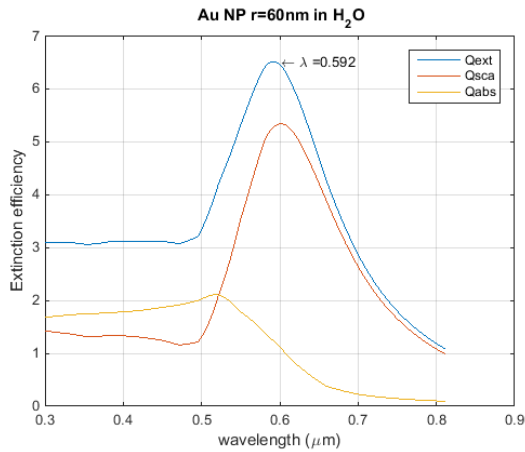


Fig. 2. Simulation for Au NP in water with size: a) 30 nm; b) 40 nm; c) 50 nm; d) 60 nm and e) 70 nm.

Results show that the increase on the particle size results in a shift of the plasmonic peak to longer wavelength range. With Au NP of 30nm the peak appears at 536 nm and with 70 nm at 622 nm. From 30 nm up to 50 nm the magnitude of the LSPR peak increases with the size, and in the range 50 nm up to 70 nm it decreases again. Thus the maximum for Au NP is observed with 50 nm at 570 nm.

In Figure 3 it is displayed the  $Q_{ext}$  variation with light wavelength for gold NP in water with sizes ranging from 30 nm up to 70 nm.

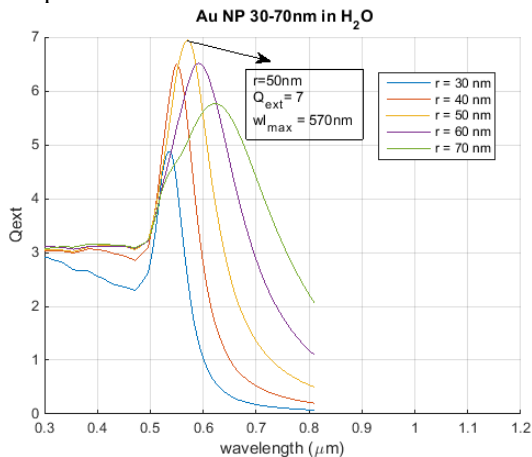


Fig. 3.  $Q_{ext}$  variation with light wavelength for Au NP in water with sizes ranging from 30 nm up to 70 nm.

Data show that the plasmonic signal occurs in the range from 540 nm to 650 nm, depending on the NP size. The increase of the NP size shifts the resonance signal to longer wavelengths and broadens the signal. The maximum resonance peak occurs at 570 nm for Au NP of 50 nm radius.

## 2. Influence of silver NP size in water

In Figure 4 it is displayed the simulated extinction coefficient variation with light wavelength for silver NP of sizes of 50 nm. This size corresponds to the size of Au NP with maximum plasmonic peak. It was assumed that NP were embedded in water. The wavelength range varied from 300 nm up to 900 nm.

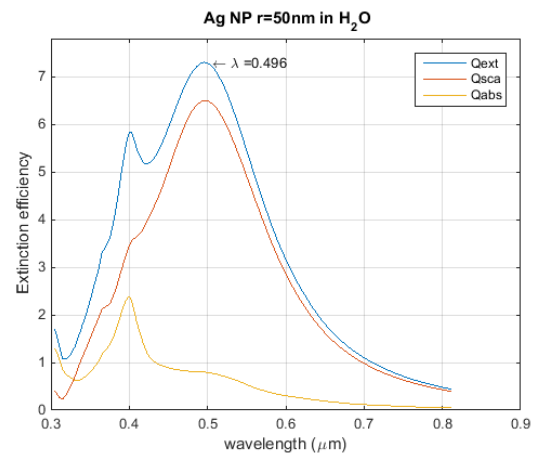


Fig. 4. Simulation for Ag NP in water with size 50 nm.

Results show that when we compare NP of the same size, the silver NP present the plasmonic peak at 496 nm, which corresponds to a shift to shorter wavelengths. Gold NP of 50 nm exhibit the plasmonic peak at 570 nm.

In Figure 5 it is displayed the  $Q_{ext}$  variation with light wavelength for silver NP in water with sizes ranging from 30 nm up to 70 nm.

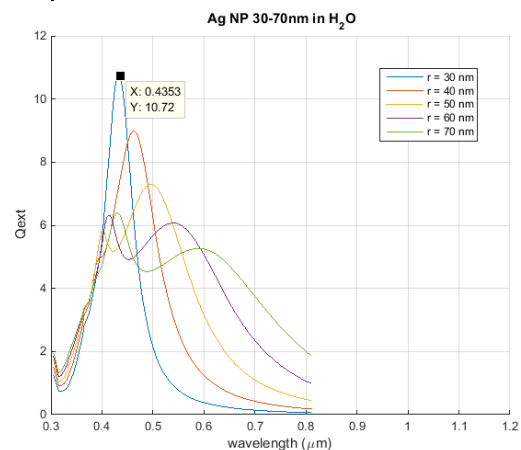


Fig. 5.  $Q_{ext}$  variation with light wavelength for Ag NP in water with sizes ranging from 30 nm up to 70 nm.

Results show that for silver NP the plasmonic signal is maximum for small size particles (30 nm). When the NP size increases it is observed that the plasmonic peak

exhibits lower magnitude, shifts to the longer values and broadens in a wider range of values.

### 3. Influence of aluminum NP size in water

In Figure 6 it is displayed the simulated extinction coefficient variation with light wavelength for aluminum NP, embedded in water, of sizes ranging from 30 nm up to 70 nm.

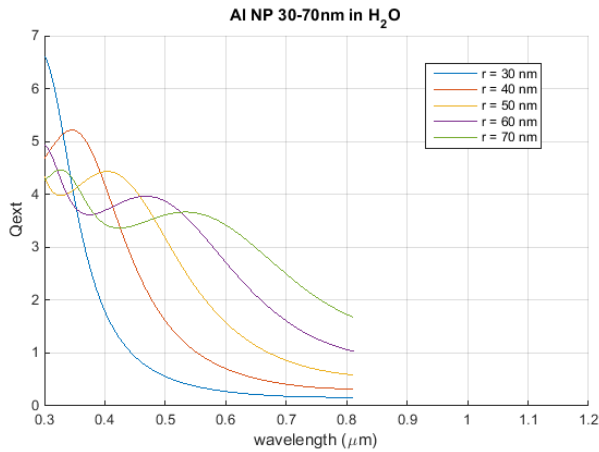


Fig. 6.  $Q_{ext}$  variation with light wavelength for Al NP in water with sizes ranging from 30 nm up to 70 nm.

In Al NP the plasmonic signal is well defined for 40 nm size. For the other NP sizes the signal is broad and of low magnitude, corresponding to a low excitation effect. As the range of interest is limited to 300 nm up to 900 nm, we will not consider particles of smaller sizes, that will provide plasmonic response at wavelengths below 300 nm.

### 4. Influence of the rGO as embedding medium

In Figure 7 it is displayed the simulation of the extinction coefficient for different metallic NP composed of gold, silver and aluminum. The NP sizes was varied in the range 30 nm – 70 nm.

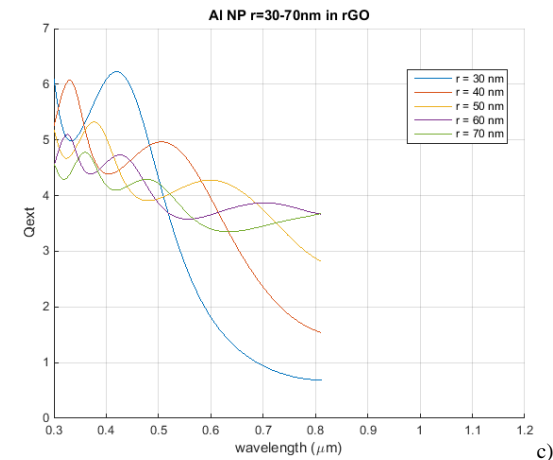
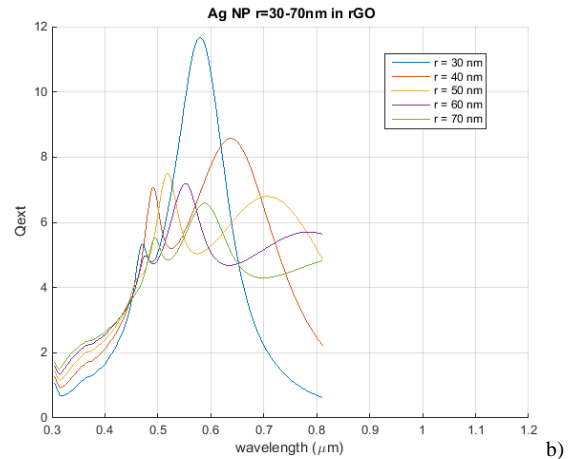
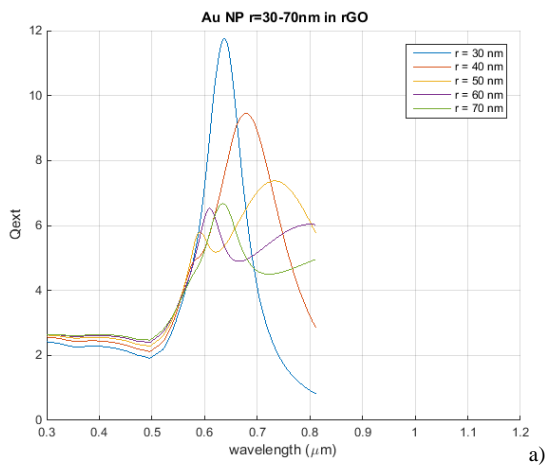


Fig. 7. Simulation of  $Q_{ext}$  for different metallic NP (sizes in the range: 30 – 70 nm) embedded in a rGO medium composed of: a) Au, b) Ag and c) Al.

Accordingly, to the simulation results it is possible to infer that the highest magnitude of the resonance peaks occurs either with gold or silver NP of 30 nm. The increase on the NP size decreases the peak magnitude. This behavior is more evident in silver than in gold. The aluminum NP produces a reduced response at the resonance wavelength and a shift of the peak to lower wavelengths range.

### 5. Influence of NP in water with a rGO mantle

In Figure 8 it is displayed a pictorial representation of the simulation conditions of the next results, where metallic NP were involved in a rGO mantle and immersed in water. Thus the embedding medium has to take into account the interaction of both rGO and water.

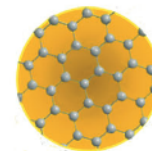
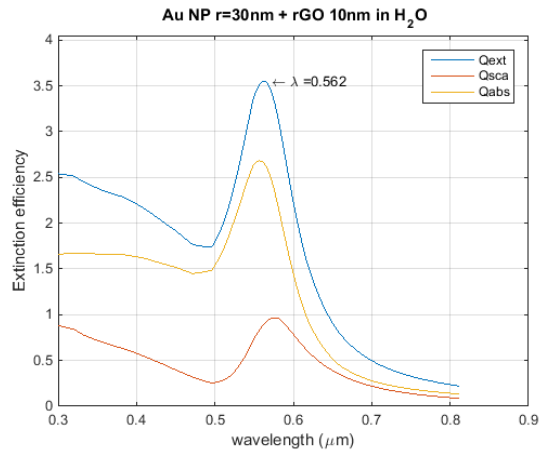
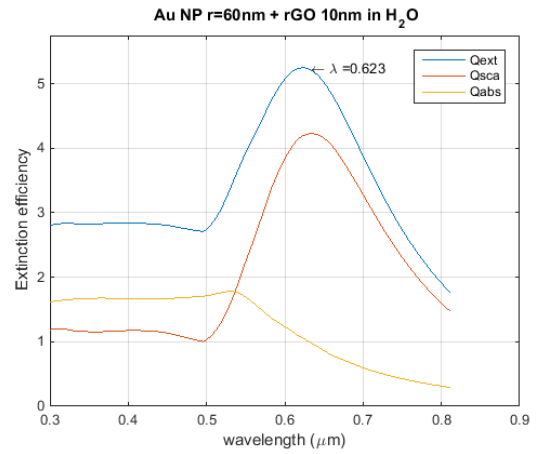


Fig. 8. Metallic NP involved in a rGO mantle.

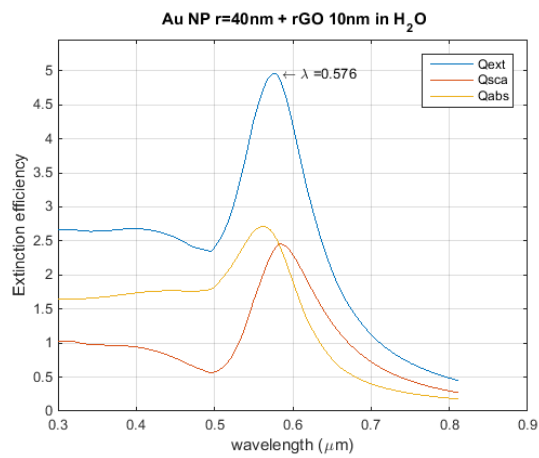
In Figure 9 it is displayed the  $Q_{ext}$  variation with light wavelength for gold NP of variable sizes immersed in water and with a rGO mantle (10 nm thick).



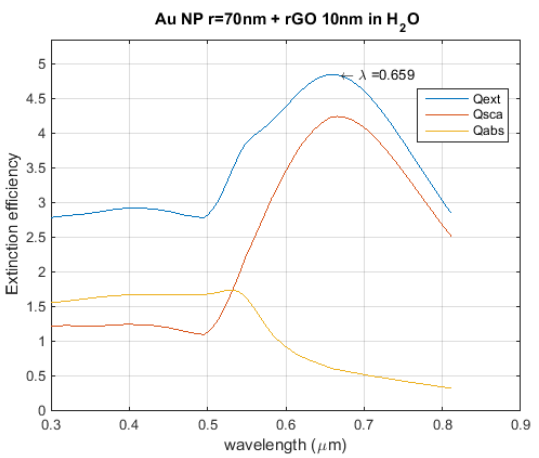
a)



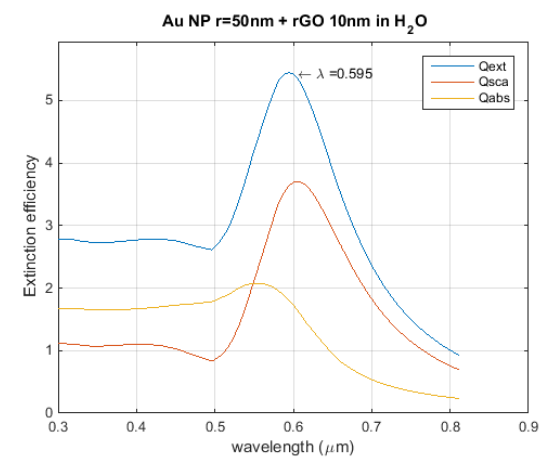
d)



b)



e)



c)

Fig. 9.  $Q_{ext}$  variation with light wavelength for gold NP in water with a rGO mantle 10 nm thick. The size of the NP is: a) 30 nm, b) 40 nm, c) 50 nm, d) 60 nm and e) 70 nm.

The introduction of rGO around the NP changes the plasmonic response. The main differences are related to the magnitude of the peak, that is reduced as well as the peak wavelength that exhibits a slight shift to longer wavelengths.

In Figure 10 it is displayed the  $Q_{ext}$  variation with light wavelength for gold NP with radius of 30 nm wrapped with a rGO mantle of variable size (10-30 nm) and immersed in water.

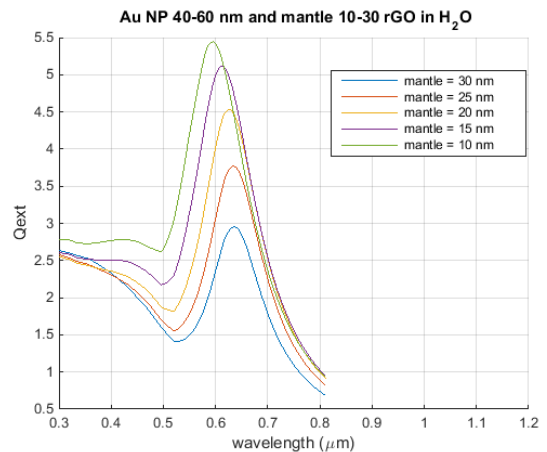


Fig. 10.  $Q_{ext}$  variation with light wavelength for gold NP of fixed size (30 nm) wrapped with a rGO mantle of variable size immersed in water.

The use of a thicker rGO mantle around the Au NP induces a strong reduction of the plasmonic peak and a shift of its spectral position to longer wavelengths. The variation of 20 nm in the mantle thickness resulted in a decrease of the plasmonic peak of 45% and a shift of 40 nm (from 600 nm to 640 nm).

In Figure 11 it is displayed the  $Q_{ext}$  variation with light wavelength for silver NP with variable radius (30-50 nm) wrapped with a rGO mantle 10 nm thick and immersed in water.

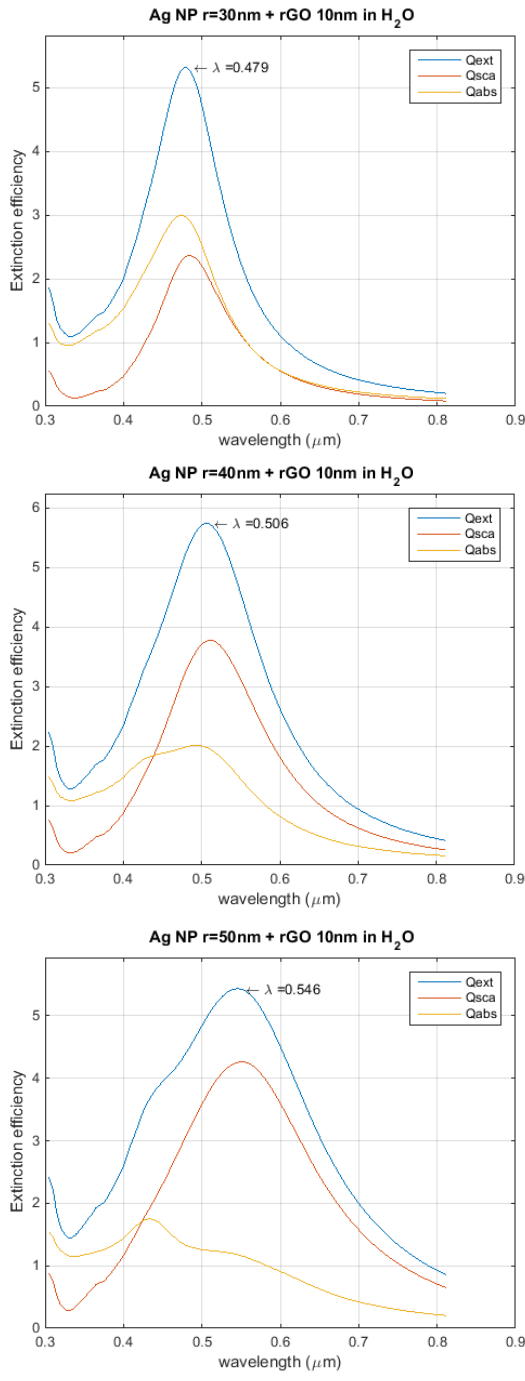


Fig. 11.  $Q_{ext}$  variation with light wavelength for silver NP of different sizes in water with a rGO mantle 10 nm thick. The size of the NP is: a) 30 nm, b) 40 nm and c) 50 nm.

The use of silver NP with the rGO mantle produces similar results to the ones obtained with gold NP. There is a reduction of the plasmonic peak magnitude when compared with silver NP of the same size immersed in water. Besides, the shift of the peak to longer wavelengths is more evident.

In Figure 12 it is displayed the  $Q_{ext}$  variation with light wavelength for silver NP, with 30 nm of radius, in water with a rGO mantle with variable thickness (0 – 20 nm).

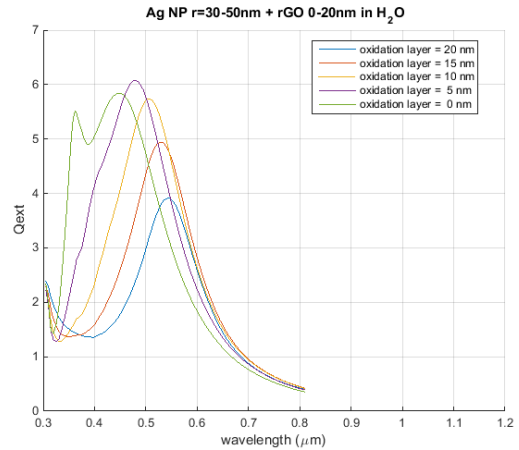
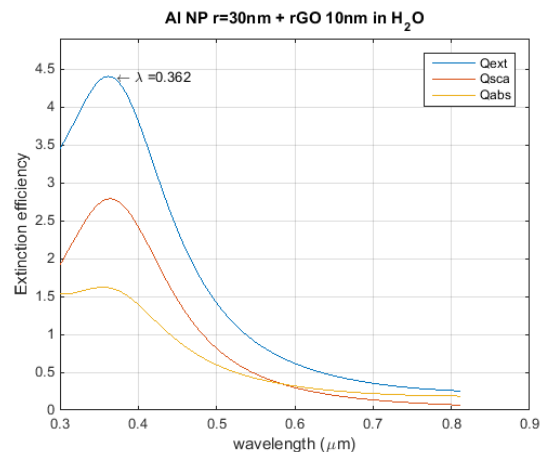


Fig. 12.  $Q_{ext}$  variation with light wavelength for silver NP with radius of 30 nm in water with a rGO mantle of variable thickness (0-20 nm).

a)

Results show the occurrence of the plasmonic peak in the blue region of the spectrum (450 nm) when the rGO mantle is not present, and a shift to longer wavelengths when the rGO wraps the NP. This shift increases with the size of the rGO mantle. At 20 nm the plasmonic peak is located near 550 nm.

In Figure 13 it is displayed the  $Q_{ext}$  variation with light wavelength for aluminum NP, with variable radius (30 nm, 40 nm and 50 nm), in water with a rGO mantle 10 nm thick.



a)

b)

c)

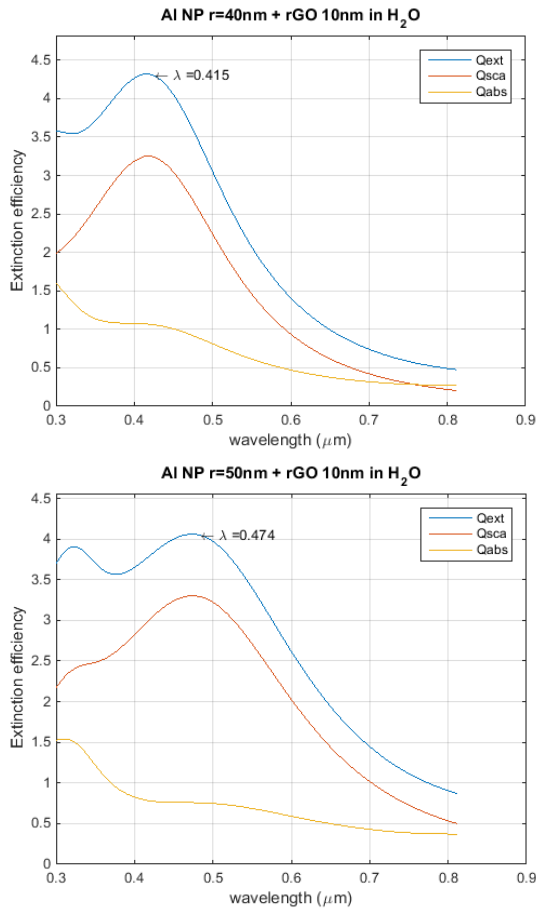


Fig. 13.  $Q_{ext}$  variation with light wavelength for aluminum NP of different sizes (a) 30 nm, b) 40 nm and c) 50 nm) in water with a rGO mantle 10 nm thick.

Results demonstrate again that the increase of the NP size shifts the plasmonic peak from the UV range (around 360 nm) to the visible range (480 nm). The magnitude of the peak exhibits a slight decrease.

In Figure 14 it is displayed the is displayed the  $Q_{ext}$  variation with light wavelength for aluminum NP, with 30 nm of radius, in water with a rGO mantle with variable thickness (0 – 20 nm).

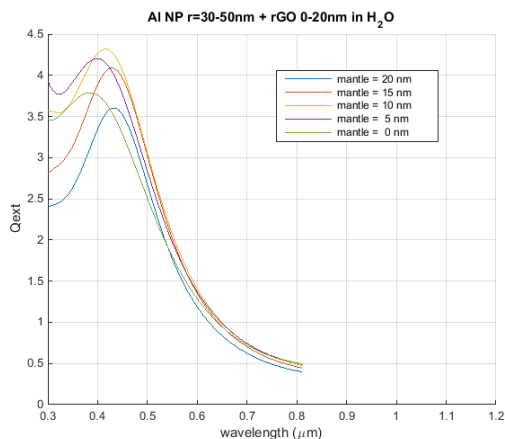


Fig. 14.  $Q_{ext}$  variation with light wavelength for aluminum NP with radius of 30 nm in water with a rGO mantle of variable thickness (0-20 nm).

The variation of the mantle dimension influences mainly the magnitude of plasmonic peak. The position in the spectral range shows a negligible variation.

## VI. CONCLUSIONS

Results obtained for NP composed of different metals, with different sizes and used in different media, show that maximum plasmonic values are strongly dependent on the following factors: size of NP, their geometry and surrounding environment, water and graphene, as medium or mantle.

It was also demonstrated that, for Au, Ag and Al NP of different sizes and different mantle thicknesses of rGO, that the wavelength  $\lambda_{LSPR}$  at which the maximum plasmonic peak occurs, depends on several factors, namely, metallic composition of the NP, size of NP's and surrounding environment (rGO).

In addition, it was concluded that the change of the environment and the change of k values caused changes in plasma maximum values  $\lambda_{LSPR}$ .

For gold NP in water, it was demonstrated that the maximum peak value  $\lambda_{LSPR}$  shifts to longer wavelengths when the size of NP increases and exhibits the maximum value for 50 nm radius at 570 nm. For silver and aluminum NP in water, it was observed that for larger particles the peaks shifted to shorter wavelengths. In NPs of Ag and Al the correspondent maximum is assigned to the smallest NP size (30 nm).

When nanoparticles are embedded into rGO as surrounding medium, it was observed a shift of the maximum peak to longer wavelengths. The same effect is observed when the metallic NP is wrapped with a rGO mantle of variable size and embedded in water. In this case it is also noted that there is also strong dependence of thickness of rGO layer regarding maximum peaks values .

In summary, the results confirmed that the maximum plasmonic peak values  $\lambda_{LSPR}$  depend on changes in refractive index and extinction between layers of NP, size of NP and variations in refractive index and extinction (dielectric function) between NP and or surrounding environment (water/rGO).

## VII. FUTURE WORK

Next steps, related to the study of functional biosensors, will have to include the addition of antibodies (AB), interaction with metallic NP as well as LSPR effects on metallic NP + rGO + AB nanostructures embedded in water. Depending on the obtained results, decisions will be taken on the possible ways to pursue the research. There are two possible directions. The study may proceed on liquid samples involving LSPR effects (current study) or may continue on the research of plasmonic effects (SPR) with solid samples deposited on the graphene layer metal surface.

## VIII. REFERENCES

- [1] de Jesus, Karla Acemano, Estevão Freire, and Maria José OC Guimarães. "Grafeno: aplicações e tendências tecnológicas." (2012).

- [2] Pei, Q. X., Y. W. Zhang, and V. B. Shenoy. "A molecular dynamics study of the mechanical properties of hydrogen functionalized graphene." *Carbon* 48.3 (2010): 898-904.
- [3] Novoselov, K. S., Geim, A. K., Morozov, S. V., Jiang, D., Zhang, Y., Dubonos, S. V., Grigorieva, I. V., Firsov, A. A. Electric field effect in atomically thin carbon films. *Science*, 306, 666-669, 2004.
- [4] Segundo, José Etimógenes Duarte Vieira, and Eudésio Oliveira Vilar. "Grafeno: Uma revisão sobre propriedades, mecanismos de produção e potenciais aplicações em sistemas energéticos." *Revista Eletrônica de Materiais e Processos* 11.2 (2016).
- [5] Khalil, Ibrahim, et al. "Graphene–gold nanoparticles hybrid—synthesis, functionalization, and application in a electrochemical and surface-enhanced raman scattering biosensor." *Materials* 9.6 (2016): 406.
- [6] Zarbin, Aldo JG, and Marcela M. Oliveira. "Nanoestruturas de carbono (nanotubos, grafeno): Quo Vadis." *Química Nova* 36.10 (2013): 1533-1539.
- [7] Turcheniuk, Kostiantyn, Rabah Boukherroub, and Sabine Szunerits. "Gold–graphene nanocomposites for sensing and biomedical applications." *Journal of Materials Chemistry B* 3.21 (2015): 4301-4324.
- [8] Ferreira, Jacqueline, et al. "Ressonância de plasmon de superfície localizado e aplicação em biossensores e células solares." *Química nova*. Vol. 39, n. 9 (Nov. 2016), p. 1098-1111 (2016).
- [9] Cittadini, Michela, et al. "Graphene oxide coupled with gold nanoparticles for localized surface plasmon resonance based gas sensor." *Carbon* 69 (2014): 452-459.
- [10] Cittadini, Michela, et al. "Graphene oxide coupled with gold nanoparticles for localized surface plasmon resonance based gas sensor." *Carbon* 69 (2014): 452-459.
- [11] Amendola, Vincenzo, et al. "Surface plasmon resonance in gold nanoparticles: a review." *Journal of Physics: Condensed Matter* 29.20 (2017): 203002.
- [12] Hergert, W, and Thomas Wriedt. *The Mie Theory: Basics and Applications*. Berlin: Springer, 2012. Internet resource.
- [13] Quinten, Michael. *Optical properties of nanoparticle systems: Mie and beyond*. John Wiley & Sons, 2010.